Articles

Intramolecular Acylolysis of Amide Derivatives of Kemp's Triacid: Strain Effects and Reaction Rates

Timothy P. Curran,*[1] Christopher W. Borysenko,[2] Susan M. Abelleira, and Renee J. Messier

Alkermes, Inc., 64 Sidney Street, Cambridge, Massachusetts 02139

Received January 25, 1994[⊗]

Intramolecular acylolysis of comparable secondary and tertiary amide derivatives of Kemp's triacid, **4**, and its *cis,trans* isomer **5** has been examined. For both triacids, the tertiary amide derivatives undergo acylolysis about 1000 times faster than the corresponding secondary amide. Also, amide derivatives of Kemp's triacid undergo acylolysis about 100 times faster than the corresponding amide derivatives of the *cis,trans* isomer. Thus, acylolysis rates spanning a range of nearly 10^6 are observed. It is proposed that the large rate difference between secondary and tertiary amides in these molecules results from greater pseudoallylic (pseudo-$A^{1,3}$) strain associated with the tertiary amides. It also is proposed that the slower acylolysis rates observed with amide derivatives of the *cis,trans* isomer of Kemp's triacid result from greater 1,3-diaxial strain associated with acylolysis of these compounds. The data show that both the structure of the triacid and the structure of the amide have a direct effect on the acylolysis rate. Because previous studies only focused on the structure of the triacid, the proposal that intramolecular acylolysis of amide derivatives of Kemp's triacid is a useful model system for studying enzyme catalysis (Menger, F. M.; Ladika, M. *J. Am. Chem. Soc.* **1988**, *110*, 6794. Menger, F. M. *Biochemistry* **1992**, *31*, 5368) is reexamined.

In 1988 the rapid acylolysis[3] of pyrrolidine amide **1** by intramolecular nucleophilic attack of a neighboring carboxylic acid to yield anhydride acid **2** and pyrrolidine (**3**) was reported.[4] For example, at pD 7.05 and 21.5 °C, **1** is

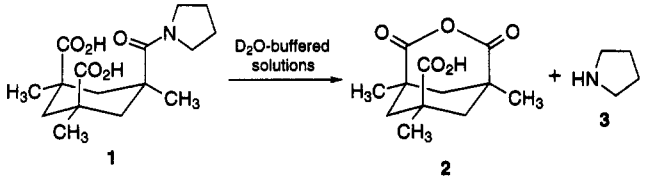

1 2 3

cleaved with $t_{1/2}$ of 7.7 min, while at pD 2.0 and 21.5 °C, the acylolysis rate is even faster, with $t_{1/2}$ being 1.7 min.[4] We thought to exploit this chemistry and employ **4** or a related species as a pH-labile reagent for the reversible coupling of drugs to protein carriers.[5] One question concerning the use of Kemp's triacid, **4**,[6] for this purpose was whether the rapid rate of reaction exhibited by **1** was typical for other amide derivatives of **4**.

To address this question, comparable secondary and tertiary amide derivatives of **4** were prepared and their acylolysis rates determined. The data show that the tertiary amide undergoes acylolysis about 1000 times faster than the secondary amide. In order to explore further this rate difference, secondary and tertiary amide derivatives of the *cis,trans* isomer of Kemp's triacid, **5**,

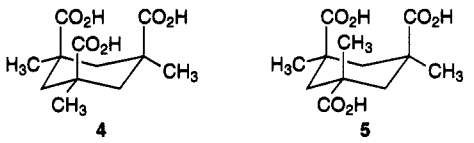

4 5

were prepared and their acylolysis rates determined. Again, the tertiary amide undergoes acylolysis about 1000 times faster than the secondary amide. In addition, it was discovered that acylolysis of a secondary amide derivative of **5** proceeds at a rate 2 orders of magnitude slower than the corresponding amide derivatives of **4**.

Results

Diacid Amide Derivatives of 4. Secondary vs Tertiary Amides. To compare secondary and tertiary amide derivatives of **4**, the diacid amides **6** and **7** were prepared. Reaction of anhydride acid **2** with phenethylamine (**8**) yielded **6**, which is stable and can be stored at 4 °C for several weeks before trace amounts of **8** become detectable. In contrast, **7**, because of its greater reactivity, had to be generated *in situ* according to the methodology previously used to examine **1**.[4] First, anhydride amide **10** was prepared by condensation of anhydride acid chloride **11** with *N*-methylphenethylamine (**9**);alkaline hydrolysis of **10** followed by acidification afforded **7**, which was used immediately for kinetic analysis. Kinetic data for intramolecular acylolysis of tertiary amide, **7** (**7** → **2** + **9**), was obtained using ^{1}H NMR; products were identified

⊗ Abstract published in *Advance ACS Abstracts,* June 1, 1994.

(1) Present address: College of the Holy Cross, Department of Chemistry, P.O. Box C, Worcester, MA 01610-2395.

(2) Present address: Brandeis University, Graduate Department of Biochemistry, 415 South Street, Waltham, MA 02254.

(3) (a) Bender, M. L. *J. Am. Chem. Soc.* **1957**, *79*, 1258. (b) Kirby, A. J.; Lancaster, P. W. *J. Chem. Soc., Perkin Trans. 1* **1972**, 1206. (c) Aldersley, M. F.; Kirby, A. J.; Lancaster, P. W. *J. Chem. Soc., Chem. Commun.* **1972**, 570. (d) Aldersley, M. F.; Kirby, A. J.; Lancaster, P. W.; McDonald, R. S.; Smith, C. R. *J. Chem. Soc., Perkin Trans. II* **1974**, 1487.

(4) Menger, F. M.; Ladika, M. *J. Am. Chem. Soc.* **1988**, *110*, 6794.

(5) Koppel, G. A. *Bioconjugate Chem.* **1990**, *1*, 13.

(6) (a) Kemp, D. S.; Petrakis, K. S. *J. Org. Chem.* **1981**, *46*, 5140. (b) Rebek, J., Jr.; Askew, B.; Killoran, M.; Nemeth, D.; Lin, F.-T. *J. Am. Chem. Soc.* **1987**, *109*, 2426. (c) Askew, B.; Ballester, P.; Buhr, C.; Jeong, K. S.; Jones, S.; Parris, K.; Williams, K.; Rebek, J., Jr. *J. Am. Chem. Soc.* **1989**, *111*, 1082. (d) Rebek, J., Jr.; Askew, B.; Ballester, P.; Doa, M. *J. Am. Chem. Soc.* **1987**, *109*, 4119.

0022-3263/94/1959-3522$04.50/0

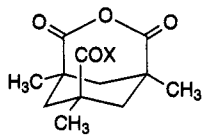

10, X = $N(CH_3)CH_2CH_2Ph$
11, X = Cl

on the basis of comparison with known samples. Data for acylolysis of secondary amide, **6** (**6** → **2** + **8**), could be obtained using ^1H NMR but was more conveniently obtained using HPLC; again, products were identified by comparison with known samples.

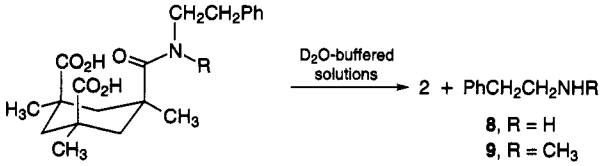

6, R = H
7, R = CH_3
8, R = H
9, R = CH_3

The pD–rate profiles for acylolysis of **6** and **7** are compared in Figure 1. The profile for **7** is similar to that reported for **1**, and the rates of acylolysis of **7** are nearly identical to those previously reported for **1** under similar conditions.[4] For example, at pD 7.0 at 22 °C, $t_{1/2}$ for **7** is 5.3 min, while for **1** at pD 7.05 at 21.5 °C, $t_{1/2}$ is 7.7 min. In contrast, the data for diacid secondary amide **6** show an acylolysis rate between 2 and 4 orders of magnitude slower than that of either **7** or **1**. For example, at pD 4.8 at 22 °C, $t_{1/2}$ for acylolysis of **6** is 10 h, while for **7** $t_{1/2}$ is 1.9 min. Thus, at this pD, the diacid tertiary amide **7** undergoes acylolysis 300 times faster than the diacid secondary amide **6**. At pD 7.0 the difference in reaction rates is even greater: $t_{1/2}$ for **6** is 270 h, while for **7** $t_{1/2}$ is 5.4 min. Thus, at pD 7.0, acylolysis of **7** proceeds nearly 3000 times faster than **6**.

Amide Acid Ester Derivative of 4. Axial Carboxylic Acid vs Axial Ester. In order to examine what effect substitutions for one of the axial carboxylic acids has on the acylolysis rate, acylolysis of secondary amide acid methyl ester **12** was examined. This compound was readily prepared by reaction of anhydride methyl ester **13** and phenethylamine (**8**). The corresponding tertiary amide acid methyl ester (which would have been prepared from reaction of **13** and **9**) was not examined, owing to difficulties we encountered in preparing and isolating this highly reactive compound. Previous work with a tertiary amide acid methyl ester derivative of **1** had shown that changing one of the carboxylic acids to an ester had very little effect on the acylolysis rate.[4] Acylolysis of **12** (**12** → **13** + **8**) was examined using HPLC; products were identified on the basis of comparison to known samples.

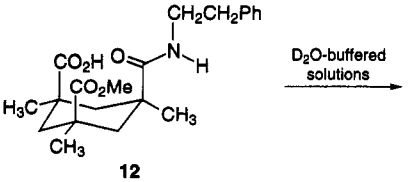

12

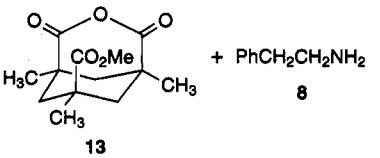

13 **8**

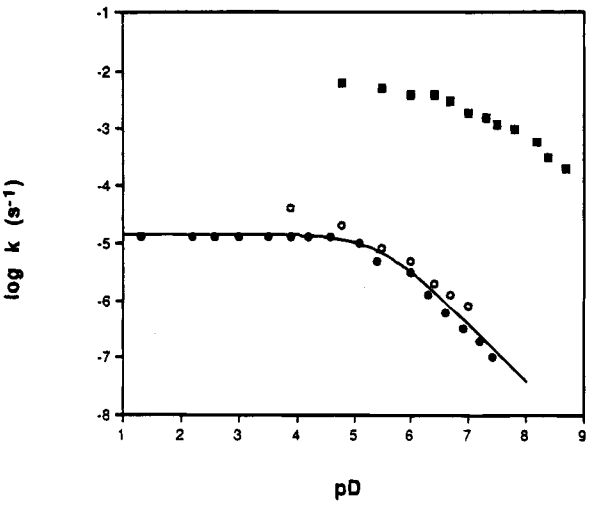

Figure 1. Plot of log k (s^{-1}) vs pD for amide acylolysis of secondary amide diacid **6** (○), tertiary amide diacid **7** (■), and secondary amide acid methyl ester **12** (●) at 22 °C. The data for **6** and **7** could not be fit to a simple mathematical model owing to complexity of the reaction arising from the presence of two carboxylic acids in these molecules. The curve drawn through the data for **12** represent eq 1, with L = hydron concentration, K_a = apparent dissociation constant for the carboxylic acid of **12**, and k_{ind} = pH independent rate constant for the hydrolysis reaction. Parameters k_{ind} ($k_{ind} = (1.38 \pm 0.01) \times 10^{-5}\ s^{-1}$) and K_a ($K_a = (3.51 \pm 0.2) \times 10^{-6}$) were evaluated by fitting the data to the above model using Enzfitter, which employs the Marquart nonlinear regression algorithm. The values given for these parameters are value ± standard error.

The pD–rate profile for this reaction is compared to those of **6** and **7** in Figure 1. The data clearly show that the rate of acylolysis for **12** is comparable to that of **6**. For example, at pD 6.0 acylolysis of **6** is only 1.6 times faster than acylolysis of **12**. Acylolysis of **12** was also examined in buffer solutions in which the buffer concentration and/or the ionic strength of the solution was varied, and no changes in reaction rate were observed. Overall, the data for acylolysis of **12** show that replacement of an axial carboxylic acid with an axial ester has a negligible effect on the reaction rate.

The rate profile for **12**, which has only one carboxylic acid, adheres nicely to eq 1

$$\log(k_{obs}) = \log[(k_{ind}L)/(K_a + L)] \qquad (1)$$

where L = hydron concentration, K_a = apparent dissociation constant for the carboxylic acid of **12**, and k_{ind} = pD independent rate constant for the acylolysis reaction. Thus, at pD > 5.5, the slope of the curve changes from 0 to −1. Such a pD–log k profile is consistent with the C–O bond-forming step being attack of a carboxylate on a protonated amide as seen in other acylolysis reactions.[3] The parameters k_{ind} ($k_{ind} = (1.38 \pm 0.01) \times 10^{-5}\ s^{-1}$) and K_a ($K_a = (3.51 \pm 0.2) \times 10^{-6}$) were calculated using a Marquart nonlinear regression algorithm on the experimental data. Unlike **12**, the rate profiles for diacids **6** and **7** do not adhere to eq 1. In particular, below pD 5 the slope of the curve does not become 0. This deviation in behavior of **6** and **7** from eq 1 is probably due to the presence of two protonated carboxylic acids in these molecules and is consistent with previous data obtained with **1**.

The fate of the Kemp's triacid moiety during acylolysis of **12** could not be easily monitored using HPLC but was more amenable to analysis using ^1H NMR. Thus, a

solution of **12** at pD 4.0 at 22 °C was examined over a 50-h period, and products were identified on the basis of the appearance of CH_3O resonances. Initially, **12** reacted to produce **8** and anhydride ester **13**, confirming that the anhydride is the initial product of the acylolysis reaction. Later, diacid ester **14** was observed to form, at the expense of **13**, demonstrating that the diacid is formed by hydrolysis of the anhydride. After 21 h the concentrations of **13** and **14** are roughly equal. Even after 50 h, no methoxy singlet for CH_3OH was observed, demonstrating that the ester does not react under conditions where acylolysis of the amide bond occurs, which is consistent with earlier observations made with a tertiary amide acid methyl ester.[4]

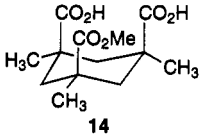

14

Amide Acid Ester Derivatives of 5. Secondary vs Tertiary Amides. To probe further the rate differences observed between secondary and tertiary amides **6** and **7**, and to examine another axial substituent, acylolyses of amide derivatives of **5**,[6c] the *cis,trans* isomer of **4**, were examined. For this triacid, amide acid esters were employed. Secondary amide derivative **15** was prepared by reaction of anhydride methyl ester **17**[7] with 3,4-dimethoxyphenethylamine (**18**). Similarly, tertiary amide derivative **16** was prepared by reaction of **17** with *N*-methyl-3,4-dimethoxyphenethylamine (**19**). Both derivatives, surprisingly even the tertiary amide, were amenable to characterization and stable to storage at 4 °C for several weeks before any traces of either **18** or **19** could be detected.

Prior to an examination of acylolysis reactions of **15** and **16**, we sought to determine whether **5** and its derivatives solely assume conformation **A** (two axial carbonyls and one axial methyl) or whether **5** can rapidly equilibrate between conformers **A** and **B**(one axial car-

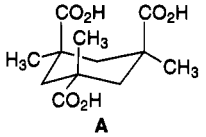

A

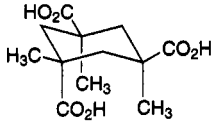

B

bonyl and two axial methyls). On the basis of the demonstrated preference for carbonyls rather than methyls to assume the triaxial positions in Kemp's triacid,[6,8] we anticipated that **A** would be the preferred conformation.

To establish this, ^1H NMR chemical shift differences between geminal axial and equatorial protons in **5** and the corresponding anhydride methyl ester **17** were examined. In the ^1H NMR spectrum of **17** in $(CD_3)_2SO$, the geminal axial and equatorial protons located between the anhydride carbonyls appear as two widely-spaced doublets at 2.2 ppm (equatorial) and 1.4 ppm (axial). Because of the ring-locked nature of **17**, the chemical shift difference between these protons is indicative of the chemical shift difference expected for **5** if it solely or predominantly

(7) The anhydride methyl ester **17** was a gift from Dr. B. Mitra Tadayoni. It was prepared from the anhydride acid (ref 6c) by treatment with CH_2N_2.

(8) Menger, F. M.; Chicklo, P. A.; Sherrod, M. J. *Tetrahedron Lett.* **1989**, *30*, 6943.

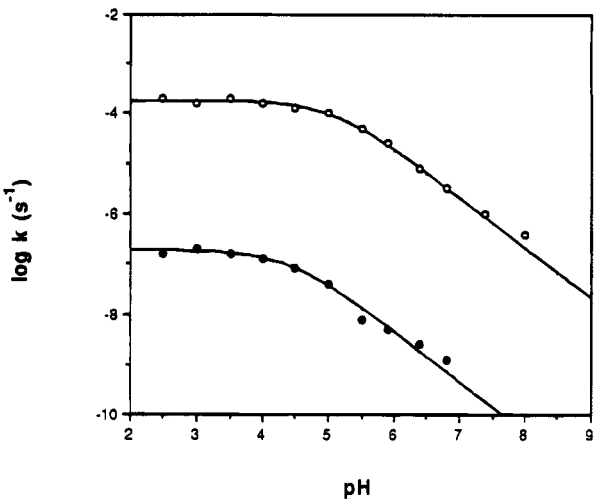

Figure 2. Plot of log k (s^{-1}) vs pH for amide acylolysis of secondary amide **15** (●) and tertiary amide **16** (○) at 22 °C. The curves represent eq 1, with L = hydron concentration, K_a = apparent dissociation constant for the carboxylic acid, and k_{ind} = pH independent rate constant for the acylolysis reaction. Parameters k_{ind} and K_a were evaluated by fitting the experimental data to eq 1 using Enzfitter, which employs the Marquart nonlinear regression algorithm. For **15**, $k_{ind} = (1.82 \pm 0.08) \times 10^{-7}$ s^{-1} and $K_a = (4.1 \pm 0.9) \times 10^{-5}$ while for **16**, $k_{ind} = (1.80 \pm 0.03) \times 10^{-4}$ s^{-1} and $K_a = (8.8 \pm 0.7) \times 10^{-6}$, where the numbers given are value ± standard error.

assumes conformation **A**. In contrast, if **5** is rapidly equilibrating between conformations **A** and **B**, then a much smaller chemical shift difference between the methylene resonances in **5** is expected.[6] The ^1H NMR spectrum of **5** in $(CD_3)_2SO$ reveals that the methylene protons sandwiched between the two *cis* carboxylic acids appear as two widely-spaced doublets at 2.4 ppm (equatorial) and 1.2 ppm (axial), and similar chemical shift differences are witnessed with **15** and **16**. Since no significant change in chemical shift difference between these axial and equatorial protons in **5**, **15**, **16**, and **17** is seen, it is likely that protonated **5** and its amide derivatives predominantly adopt conformation **A** in solution. Thus, **15** and **16** are maintained in a conformation that can allow nucleophilic attack of a neighboring carboxylic acid on the amide.

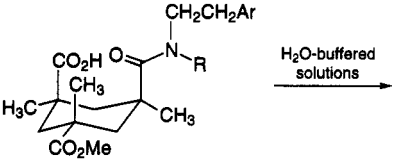

15, R = H
16, R = CH_3

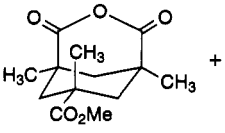

17

+ $ArCH_2CH_2NHR$
Ar = 3,4-dimethoxyphenyl
18, R = H
19, R = CH_3

Acylolysis rates for **15** (**15** → **17** + **18**) and **16** (**16** → **17** + **19**) were determined at 22 °C in appropriate buffer solutions using an HPLC assay. The pH–rate profiles for acylolysis of **15** and **16** are presented in Figure 2. The data in this graph also can be analyzed using eq 1 in order to obtain k_{ind} and K_a. For **15**, $k_{ind} = (1.82 \pm 0.08) \times 10^{-7}$ s^{-1} and $K_a = (4.1 \pm 0.9) \times 10^{-5}$ while for **16**, k_{ind} = (1.80

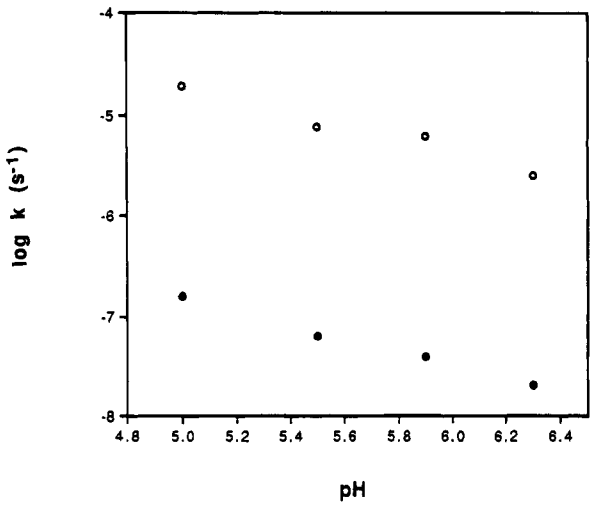

Figure 3. Plot of log k (s^{-1}) vs pH for amide acylolysis of secondary amide **15** (●) and secondary amide **20** (○) in buffered H_2O solutions at 37 °C.

$\pm 0.03) \times 10^{-4}$ s^{-1} and $K_a = (8.8 \pm 0.7) \times 10^{-6}$. In the pH range examined, acylolysis of **16** proceeds 3 orders of magnitude faster than acylolysis of **15**. For example, in the pH region where the reaction rate is invariant, **16** undergoes acylolysis 1000 times faster than **15**.

Amide Acid Ester Derivatives of 4 and 5. Axial Carboxylic Acid vs Axial Methyl. One striking feature of amide cleavage from **15** and **16** is that it occurs much slower than amide cleavage from **6** and **7**, respectively. In order to quantitate the rate difference between similar amides derived from **4** and **5**, we compared acylolyses of **15** and **20** (prepared by reaction of anhydride methyl ester **13** with **18**) at 37 °C between pH 5.0 and 6.3. Because of the slow rate of acylolysis exhibited by **15**, a higher temperature was used in order to expedite data collection. Data for acylolysis of **15** (**15** → **17** + **18**) and **20** (**20** → **13** + **18**)are given in Figure 3. The data show that acylolysis

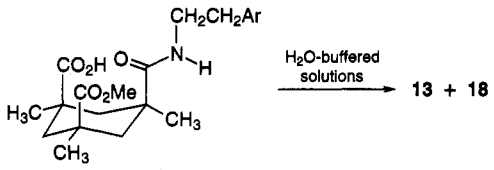

20, Ar = 3,4-dimethoxyphenyl

of **15** is 2 orders of magnitude slower than acylolysis of **20**. For example, at pH 5.0 amide cleavage from **15** is 150 times slower than amide cleavage from **20**.

Discussion

There are two main observations made from the present work. First, there is about a 1000-fold rate difference between secondary and tertiary amide derivatives of **4** and **5** (**6** compared to **7** and **15** compared to **16**). Second, amide derivatives of **5** are less reactive than amide derivatives of **4** (**15** compared to **20**).

The large rate differences between **6**–**7**, and between **15**–**16**, are striking. Intermolecular, dilute acid-catalyzed hydrolyses of comparable secondary and tertiary amides have shown that the tertiary amide undergoes hydrolysis only 1.1 times faster than the secondary amide.[9] For intramolecular amide acylolyses, there was only a 10-fold rate difference reported for acylolysis of structurally unrelated secondary and tertiary amides in a cyclohexane diacid system related to **4** and **5**,[10] and in a maleamic acid system there was only a 43-fold rate difference between comparable secondary and tertiary amides.[3d]

Previous work with the diacid pyrrolidine amide **1** had concluded that the rate acceleration observed with that compound was primarily due to proximity of the neighboring carboxylic acid and secondarily to relief of 1,3-diaxial strain.[4] Assuming this to be true, then only a small rate difference between secondary and tertiary amides should be expected. However, the large rate differences observed here indicates that, in addition to proximity and 1,3-diaxial strain relief, another factor associated with the structure of the amide (and the changes it undergoes in the reaction) contributes to the rate acceleration. Examination of space-filling models of **6**, **7**, **15**, and **16** revealed the presence of pseudoallylic (pseudo-$A^{1,3}$) strain associated with the amide, which arises from unfavorable nonbonded interactions between the amide N-substituents *trans* to the C=O bond and the alkyl substituents on the teritary cyclohexane carbon α to the amide (Figure 4).[11] In the case of the secondary amide, pseudo-$A^{1,3}$ strain results from nonbonded interactions between the *trans*-NH of the amide and the alkyl substituents on the cyclohexane carbon α to the amide (Figure 4A). In the case of the tertiary amide, pseudo-$A^{1,3}$ strain results from nonbonded interactions between the *trans*-*N*-methyl of the amide and the alkyl substituents on the cyclohexane carbon α to the amide (Figure 4B). Inspection of the models suggests that the nonbonded interactions associated with the tertiary amide in **7** and **16** may be large enough to cause distortion of the amide bond, which is known to accelerate amide hydrolysis.[12]

Pseudo-$A^{1,3}$ strain in these molecules will contribute to the rate acceleration only if it is relieved in the transition state of the reaction. The likely mechanism for this reaction, based on the similarity in reaction profiles of **12**, **15**, and **16** and other acylolysis reactions,[3] involves formation of tetrahedral intermediates such as **21** and **22**, through attack of a neighboring carboxylate on the protonated amide, followed by collapse of the intermediate to yield the amine and anhydride. Although the rate-determining step in these reactions is unknown, the transition state must certainly involve a change in hybridization at the amide carbonyl carbon from sp^2 to sp^3. As an approximation, the transition state is likely to

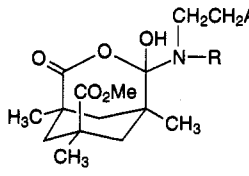

21

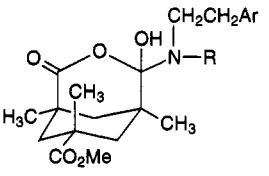

22

Ar = 3,4-dimethoxyphenyl

resemble **21** or **22**, with the amide C and N atoms taking on sp^3 hybridizations and adopting tetrahedral geometries, with concomitant lengthening of the C—N bond. These changes should alleviate pseudo-$A^{1,3}$ strain by moving the atoms in close contact away from one another.

(9) Bolton, P. D. *Aust. J. Chem.* **1966**, *19*, 1013.

(10) Menger, F.M.; Ladika, M. *J. Org. Chem.* **1990**, *55*, 3006.

(11) Johnson, F. *Chem. Rev.* **1968**, *68*, 375.

(12) Bennet, A. J.; Wang, Q.-P.; Slebocka-Tilk, H.; Somayaji, V.; Brown, R. S.; Santarieso, B. D. *J. Am. Chem. Soc.* **1990**, *112*, 6383.

(13) Turner, R. B.; Nettleton, D. E.; Perelman, M. *J. Am. Chem. Soc.* **1958**, *80*. 1430.

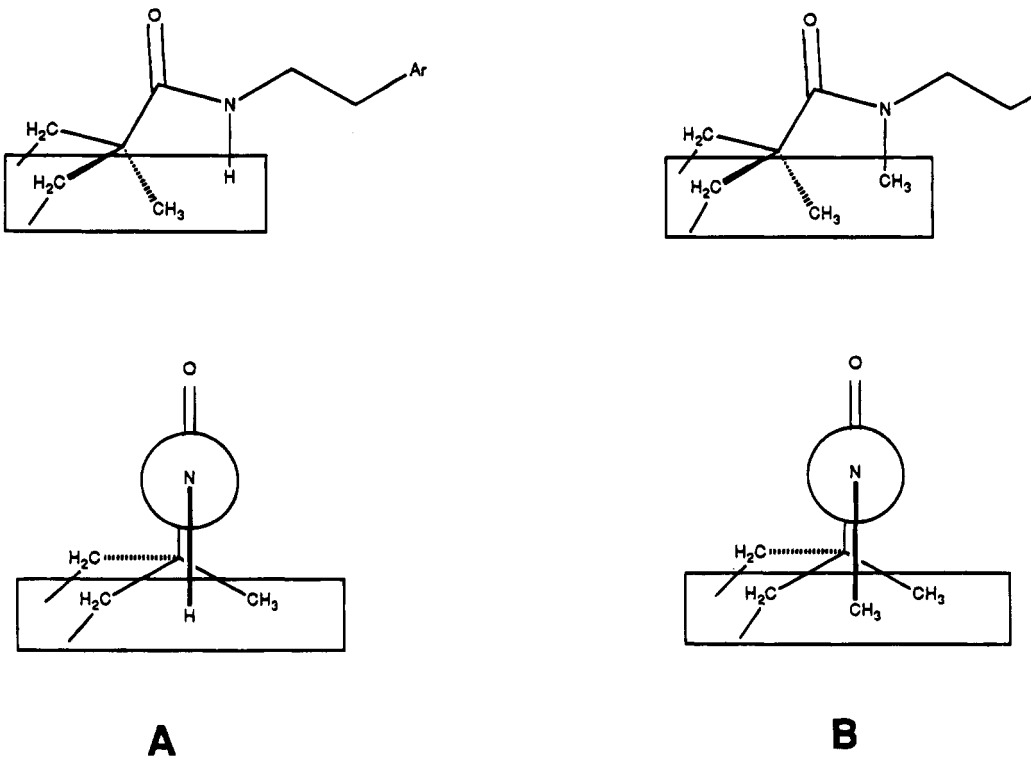

Figure 4. (A) Two perspectives illustrating the site of pseudo-$A^{1,3}$ strain (boxed area) between the amide NH and the alkyl substituents of the α, quatenary cyclohexane carbon in **6**, **13**, and **15**. (B) Two perspectives illustrating the site of pseudo-$A^{1,3}$ strain (boxed area) between the amide N—CH_3 and the alkyl substituents of the α, quatenary cyclohexane carbon in **7** and **16**.

Assuming that the rate differences between **6**–**7**, and between **15**–**16**, are derived primarily from differences in pseudo-$A^{1,3}$ strain, then these differences should be equal to the difference in the free energy of activation between **6**–**7** and between **15**–**16**. Using the data in Figure 1, the difference in the free energy of activation between **6** and **7** at pD 4.8 is 3.3 kcal/mol, while at pD 7.0 it is 4.7 kcal/mol. Using the data in Figure 3, the difference in the free energy of activation between **15** and **16** at pH 2.5 is 4.1 kcal/mol, while at pH 6.8 it is 4.5 kcal/mol. On the basis of these calculations, there appears to be about a 3–5 kcal/mol difference in pseudo-$A^{1,3}$ strain between **6**–**7** and **15**–**16**. This estimate of the difference in pseudo-$A^{1,3}$ strain correlates very well with the 4.3 kcal/mol difference in $A^{1,3}$ strain between the alkenes **23** (analogous to the tertiary amides) and **24** (analogous to the secondary amides),as determined from heats of hydrogenation.[13] Also

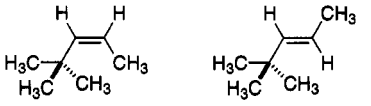

23 **24**

correlating well with our data is the 4.8 kcal/mol difference in the barrier to amide bond rotation for *N,N*-dimethylisobutyramide (**25**, analogous to the secondary amides) and *N,N*-dimethylpivalamide (**26**, analogous to the tertiary amides), as determined using NMR.[14] Both amide bond rotation and amide acylolysis go through similar transition

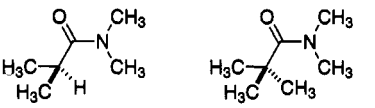

25 **26**

states, with the amide C and N atoms assuming sp^3 hybridizations and tetrahedral geometries, with concomitant adoption of tetrahedral geometries and lengthening of the C—N bond.

The rate difference between **15** and **20** is also striking, since it has to arise from replacement of the axial methyl ester in **20** with an axial methyl group in **15**. Based on the conformational analysis of **5**, it is unlikely that the observed rate deceleration observed with **15** relative to **20** results from adoption of unfavorable conformations by the cyclohexane framework of **15**. One possible explanation for the faster rate of reaction for **20** as compared to **15** is that the axial ester carbonyl in **20** stabilizes the acylolysis transition state through hydrogen-bond formation, while **15**, with an axial methyl group, cannot stabilize the transition state in any way. If this explanation is true, then the acylolysis rate should vary only if the hydrogen-bonding capacity of the third axial substituent is altered; structural changes that do not alter hydrogen-bonding capacity should not lead to any significant rate changes. Data reported previously for acylolysis of **1**[4] and **27**,[10] as well as the present data for acylolysis of **16**, do not

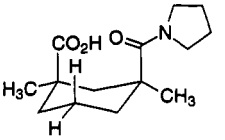

27

support this explanation. Of these three tertiary amides,

(14) Drakenberg, T.; Dahlqvist, K.-J.; Forsen, S. *J. Phys. Chem.* **1972**, *76*, 2178.

(15) The *A* values for sp^2-hybridized carbons are smaller than the *A* values for sp^3-hybridized carbons: Hirsch, J. A. *Top. Stereochem.* **1967**, *1*, 204. Also, the strain of having two 1,3-diaxial methyl groups has been measured as 3.7 kcal/mol: Allinger, N. L.; Miller, M. A. *J. Am. Chem. Soc.* **1961**, *83*, 2145.

(16) Kirby, A. J. *Adv. Phys. Org. Chem.* **1980**, *17*, 183.

only **1** has an axial carbonyl group capable of hydrogen bonding; both **16** (axial CH_3) and **27** (axial H) lack any hydrogen-bonding capacity. At pD 7.05 and 21 °C, **1** undergoes acylolysis with $t_{1/2}$ of 7.7 min, while at pD 6.90 and 21 °C **27** undergoes acylolysis with $t_{1/2}$ of 19 min. Even taking into account the pD difference, it is clear that **27** reacts slower than **1**, but only by a factor of about 4 or 5. In contrast, **16** at pH 7.0 and 22 °C undergoes acylolysis with $t_{1/2}$ of 4800 min, which is about 500 times slower than acylolysis of either **1** or **27**. The data clearly indicate that, although a third axial carbonyl group can accelerate the acylolysis reaction, its effect is relatively small and cannot be the prime reason why amide derivatives of **5** undergo acylolysis so much slower as compared to amide derivatives of **4**.

Most likely, the rate deceleration observed with **15** relative to **20** arises from destabilization of the tetrahedral intermediate of the acylolysis reaction by the axial methyl group. Consider tetrahedral intermediates **21** and **22** (R = H), derived from acylolyses of **20** and **15**, respectively. In **22** there are two sp^3-hybridized axial carbons and one sp^2-hybridized axial carbon, while in **21** there is only one sp^3-hybridized axial carbon and two sp^2-hybridized axial carbons. As noted in the conformational analysis of **5** described above and in the conformational analyses of **4**,[6,8] the most stable conformation for these cyclohexanes places the greatest number of sp^2-hybridized carbons in the 1,3-diaxial positions and avoids having two sp^3-hybridized carbons in 1,3-diaxial positions.[15] Consequently, it should be more difficult to form **22** (two 1,3-diaxial sp^3-hybridized carbons) from **15** than it is to form **21** (one axial sp^3-hybridized carbon) from **20**. The result is a slower acylolysis rate for **15** as compared to **20** (Figure 3).

Overall, the acylolyses of amide derivatives of **5** feature a competition between two strain effects. Relief of ground-state pseudo-$A^{1,3}$ strain is opposed by introduction of transition-state 1,3-diaxial strain. The results of this competition are slower acylolysis rates for amide derivatives of **5**, as compared to amide derivatives of **4**.

Conclusions

Previously, the effective molarity (EM) for the rapid acylolysis of **1** was estimated to be $>10^{14}$ M.[4] It was also concluded that there were only two sources for the rate acceleration witnessed with this reaction, 1,3-diaxial strain relief and proximity; pseudo-$A^{1,3}$ strain relief was not considered.[4] Since it was estimated that 1,3-diaxial strain relief could only contribute 10^2-10^3 toward the rate acceleration, the remainder of the rate acceleration was attributed to proximity.[4] The present results show that the structure of the amide plays a critical role in the rate acceleration witnessed with **1** and **7**, and it is proposed that it does so by relief of pseudo-$A^{1,3}$ strain associated with the amide. Using the rate differences between secondary and tertiary amide derivatives as a guide, the contribution of pseudo-$A^{1,3}$ strain relief to the rate acceleration is thought to be at least 10^3. As such, the contribution of total strain relief to the rate acceleration for **1** and **7** is minimally 10^5-10^6. Assuming that the EM for acylolysis of **1** and **7** is 10^{14} M, the contribution of proximity to the rate acceleration would be 10^8-10^9, which is 10^3 lower than previously thought.

The contribution of proximity to the rate enhancement hinges on the relevancy of the EM estimate. As noted by Kirby, there are two stringent requirements for determination of accurate EM values.[16] First, the mechanisms for both the intermolecular and intramolecular reactions being compared must be the same. Second, both the intermolecular and intramolecular reactions must be carried out under the same conditions. The EM estimate for acylolysis of **1** was based on comparison with the intermolecular hydrolysis of *N*-methylacrylamide in formic acid solutions. Although this reaction is appropriate as an intermolecular reference for acylolysis of maleamic acid derivatives, it is inappropriate for acylolysis of **1** for two reasons. First, the two amides are electronically dissimilar; *N*-methylacrylamide is a conjugated amide, and **1** is not. Secondly, *N*-methylacrylamide is a secondary amide and does not have the pseudo-$A^{1,3}$ strain present in tertiary amide **1**. For both these reasons, the $>10^{14}$ M EM estimate is highly suspect, and until an appropriate intermolecular reaction is discovered, a precise EM for these acylolysis reactions will remain unknown. As such, the exact contribution of proximity to the rate enhancement will also remain unknown.

The ambiguity concerning the contribution of proximity to the rate acceleration for acylolysis of **1** also means that interpretations of this reaction as an enzyme model need to be readdressed.[4,17] Based on the initial work with **1**, it was concluded that if an enzyme positioned one of its carboxyls adjacent to an amide substrate with the geometry provided by Kemp's triacid, little additional catalytic power would be required to achieve an enzyme-like rate enhancement. The data presented here indicate a larger contribution by strain relief and a smaller contribution by proximity to the rate acceleration than previously thought. Consequently, the rapid reaction of **1** or **7** does not support the conclusion that proper positioning of functional groups is sufficient to achieve enzymatic rate enhancements. Instead, enzymes are likely to employ a variety of methods to achieve their rate accelerations, and introduction of strain and its relief in the transition state has been noted with several enzymes.[18] On the basis of the present results, intramolecular amide acylolysis in **1** and **7** appears to model this behavior.

Finally, the data presented here illustrate that **4** and **5** can be used as molecular laboratories for the study of strain effects on reaction rates. The data also show that amide cleavage from **4** and **5** can vary by as much as 10^6, depending on the structure of the amine and the structure of the triacid. As for the use of **4** or **5** as pH-labile reagents for coupling drugs to proteins, the variable rates of the acylolysis reaction suggest that these triacids and their derivatives could be used to match amine release and pharmacokinetics. Further exploration of **4** and **5** and their structural relatives is likely to provide a greater range of amine release rates and an increased understanding of the factors which govern these intramolecular reactions.

Experimental Section

NMR spectra were obtained on a Bruker AM-250, AM-300, or AM-400 spectrometer using tetramethylsilane as the internal standard, unless otherwise noted. HPLC work was performed on a Hewlett-Packard HP-1090 HPLC equipped with a diode-array detector and a temperature-regulated autosampler. Elemental analyses were performed by Galbraith Laboratories, Knoxville, TN, or Oneida Research Services, Whitesboro, NY. TLC was performed on Merck, precoated, silica gel 60 plates.

(17) Menger, F. M. *Biochemistry* **1992**, *31*, 5368.
(18) Jencks, W. P. *Adv. Enzymol.* **1975**, *43*, 219.

Flash chromatography was performed using Aldrich 230–400-mesh silica gel. All reagents and solvents are reagent grade, unless otherwise noted.

Secondary Amide Diacid 6. To a suspension of 130 mg (0.542 mmol, 1.0 equiv) of **2**[6c] and 103 mg (0.650 mmol, 1.2 equiv) of phenethylamine hydrochloride in 2 mL of CH_2Cl_2 at 22 °C was added 0.304 mL (2.17 mmol, 4.0 equiv) of Et_3N. The resulting solution stirred for 16 h, after which it was diluted with 50 mL of CH_2Cl_2 and washed with 3 × 10 mL of 1 N HCl and 1 × 10 mL of brine. The CH_2Cl_2 layer was dried ($MgSO_4$), filtered, and evaporated to an oil. Crystallization from CH_2Cl_2/Et_2O yielded 118 mg (60%) of pure **6**: ^1H NMR (300 MHz, $CDCl_3$) δ 7.35–7.15 (5H, m, C_6H_5), 7.08 (1H, t, J = 5.1 Hz, NH), 3.40–3.34 (2H, m, N–CH_2), 2.88–2.80 (4H, m, CH_2Ph and 2 eq CH), 2.55 (1H, d, J = 14 Hz, eq CH), 1.21 (6H, s, 2 CH_3), 1.20 (3H, s, CH_3), 1.10 (1H, d, J = 14 Hz, ax CH), 1.00 (2H, d, J = 14 Hz, 2 ax CH); TLC, R_f 0.70 (1:1 EtOAc/MeOH).

Anal. Calcd for $C_{20}H_{27}NO_5$: C, 66.46; H, 7.53; N, 3.88. Found: C, 66.52; H, 7.88, N, 3.91.

Tertiary Amide Anhydride 10. To a suspension of 451 mg (1.75 mmol, 1.0 equiv) of anhydride acid chloride **11**[6a] in 40 mL of CH_2Cl_2 at 22 °C were added 0.736 mL (5.24 mmol, 3.0 equiv) of Et_3N and 248 mg (1.84 mmol, 1.1 equiv) of *N*-methylphenethylamine (**9**). The resulting solution stirred for 30 min and then was washed with 3 × 30 mL of 1 N HCl and 1 × 30 mL of brine. The CH_2Cl_2 layer was dried ($MgSO_4$), filtered, and evaporated. The off-white solid that remained was recrystallized from toluene to yield 380 mg (61%) of pure **10**: ^1H NMR (300 MHz, $CDCl_3$) δ 7.35–7.15 (5H, m, C_6H_5), 3.49 (2H, t, J = 7.6 Hz, N–CH_2), 2.94 (3H, s, N–CH_3), 2.90–2.85 (4H, m, CH_2Ph and 2 eq CH), 2.02 (1H, d, J = 13 Hz, eq CH), 1.36 (6H, s, 2 CH_3), 1.36 (1H, d, J = 13 Hz, ax CH), 1.27 (3H, s, CH_3), 1.21 (2H, d, J = 14 Hz, 2 ax CH); TLC, R_f 0.82 (EtOAc).

Anal. Calcd for $C_{21}H_{27}NO_4$: C, 70.56; H, 7.62; N, 3.92. Found: C, 70.65; H, 7.67; N, 3.83.

***In Situ* Preparation of Tertiary Amide Dicarboxylate 7.** To a solution of 2.0 mg (5.6 μmol, 1.0 equiv) of **10** in 25 μL of CD_3CN at 22 °C was added 25 μL of 0.472 M NaOD in D_2O. The resulting solution was dissolved in 0.5 mL of CD_3CN. After 5 min the ^1H NMR spectrum showed complete conversion of **10** to the dicarboxylate salt of **7**; no other products were detected by ^1H NMR. **7**: ^1H NMR (300 MHz, CD_3OD/NaOD, reference to CD_3 peak) δ 7.25–7.05 (5H, m, C_6H_5), 3.46 (2H, br s, N–CH_2), 2.96 (3H, s, N–CH_3), 2.80 (2H, m, CH_2Ph), 2.69 (2H, d, J = 14 Hz, 2 eq CH), 2.51 (1H, d, J = 14 Hz, eq CH), 1.30–1.20 (3H, m, 3 ax CH), 1.22 (3H, s, CH_3), 1.15 (6H, s, 2 CH_3).

Secondary Amide Acid Ester 12. To a suspension of 101 mg (0.400 mmol, 1.0 equiv) of anhydride methyl ester **13**[6d] and 70.0 mg (0.441 mmol, 1.1 equiv) of phenethylamine hydrochloride in 3 mL of CH_2Cl_2 at 22 °C was added 0.14 mL (1.0 mmol, 2.5 equiv) of Et_3N. After being stirred for 5 h, the reaction solution was diluted with 20 mL CH_2Cl_2 and washed with 3 × 5 mL of 1 N HCl and 1 × 5 mL of brine. The CH_2Cl_2 layer was dried ($MgSO_4$), filtered, and evaporated to yield 119 mg (80%) of pure **12** as an amorphous solid: ^1H NMR (300 MHz, $CDCl_3$) δ 7.8 (1H, br s, NH), 7.35–7.15 (5H, m, C_6H_5), 3.55 (3H, s, OCH_3), 3.52–3.22 (2H, m, N–CH_2), 2.90–2.60 (5H, m, CH_2Ph and 3 eq CH), 1.28 (3H, s, CH_3), 1.22 (3H, s, CH_3), 1.15 (3H, s, CH_3), 1.08–0.98 (3H, m, 3 ax CH); TLC, R_f 0.75 (5:1 EtOAc/MeOH).

Anal. Calcd for $C_{21}H_{29}NO_5$: C, 67.15; H, 7.79; N, 3.73. Found: C, 67.10; H, 7.99; N, 3.68.

***Cis,trans* Secondary Amide Acid Ester 15.** To a suspension of 106 mg (0.417 mmol, 1.0 equiv) of anhydride methyl ester **17**[7] in 1 mL of CH_2Cl_2 at 22 °C was added 0.155 mL of 3,4-dimethoxyphenethylamine (**18**). After 20 h of stirring, the solution was diluted with 50 mL of CH_2Cl_2 and washed with 3 × 5 mL of 1 N HCl. The CH_2Cl_2 was dried ($MgSO_4$), filtered, and evaporated to yield a white solid. Recrystallization from CH_2Cl_2/Et_2O/hexane afforded 121 mg (67%) of pure **15**: ^1H NMR (300 MHz, $CDCl_3$) δ 6.80 (1H, d, J = 8.7 Hz, aromatic CH), 6.73 (2H, m, aromatic CH), 6.57 (1H, t, J = 5.4 Hz, NH), 3.87 (3H, s, OCH_3), 3.86 (3H, s, OCH_3), 3.67 (3H, s, CO_2CH_3), 3.45 (2H, m, N–CH_2), 2.74 (2H, t, J = 7.2 Hz, CH_2Ar), 2.64 (1H, d, J = 15 Hz, eq CH), 2.32 (1H, d, J = 14 Hz, eq CH), 2.22 (1H, d, J = 14 Hz, eq CH), 1.75 (1H, d, J = 14 Hz, ax CH), 1.70 (1H, d, J = 14 Hz, ax CH), 1.27 (3H, s, CH_3), 1.26 (1H, d, J = 15 Hz, ax CH), 1.16 (3H, s, CH_3), 1.06 (3H, s, CH_3).

Anal. Calcd for $C_{23}H_{33}NO_7$: C, 63.43; H, 7.64; N, 3.22. Found: C, 63.69; H, 7.89; N, 3.22.

***Cis,trans* Tertiary Amide Acid Ester 16.** To a suspension of 100 mg (0.393 mmol, 1.0 equiv) of **17**[7] in 2 mL of CH_2Cl_2 at 22 °C was added a solution of 0.218 mL (1.18 mmol, 3.0 equiv) of *N*-methyl-3,4-dimethoxyphenethylamine (**19**) in 1 mL CH_2Cl_2. After being stirred for 22 h, the reaction solution was diluted with 25 mL of CH_2Cl_2 and washed with 3 × 5 mL of 1 N HCl and 1 × 5 mL of brine. The CH_2Cl_2 layer was dried ($MgSO_4$), filtered, and evaporated to yield a white solid. Flash chromatography (9:1 EtOAc/MeOH) afforded 67 mg (38%) of **16** as an amorphous white solid containing 0.5 molar equiv of H_2O: ^1H NMR (300 MHz, $CDCl_3$) δ 6.82–6.75 (3H, m, aromatic CH), 3.88 (3H, s, OCH_3), 3.86 (3H, s, OCH_3), 3.68 (3H, s, CO_2CH_3), 3.10 (3H, s, N–CH_3), 3.10–2.80 (2H, m, N–CH_2), 2.29 (1H, d, J = 16 Hz, eq CH), 2.10–1.90 (4H, m, CH_2Ar, 2 eq CH), 1.30–1.12 (2H, m, ax CH), 1.29 (3H, s, CH_3), 1.20 (3H, s, CH_3), 1.13 (3H, s, CH_3) 1.06 (1H, d, J = 16 Hz, ax CH); TLC, R_f 0.68 (9:1 EtOAc/MeOH).

Anal. Calcd for $C_{24}H_{35}NO_7 \cdot 0.5H_2O$: C, 62.86; H, 7.91; N, 3.05. Found: C, 62.85; H, 7.82; N, 2.91.

Secondary Amide Acid Ester 20. To a suspension of 114 mg (0.449 mmol, 1.0 equiv) of anhydride methyl ester **13**[6d] in 1 mL of CH_2Cl_2 at 22 °C was added 0.166 mL (0.985 mmol, 2.2 equiv) of **18**. After being stirred for 20 h, the solution was diluted with 50 mL of CH_2Cl_2 and washed with 3 × 5 mL of 1 N HCl. The CH_2Cl_2 layer was dried ($MgSO_4$), filtered, and evaporated to a light yellow oil. Purification by flash chromatography (9:1 EtOAc/MeOH) afforded 63 mg (32%) of pure **20** as an amorphous white solid: ^1H NMR (300 MHz, $CDCl_3$) δ 7.7 (1H, br s, NH), 6.78 (1H, s, aromatic CH), 6.75 (2H, s, aromatic CH), 3.86 (3H, s, OCH_3), 3.84 (3H, s, OCH_3), 3.60 (3H, s, CO_2CH_3), 3.40–3.25 (2H, m, N–CH_2), 2.90–2.60 (5H, m, 3 eq CH, CH_2Ar), 1.20 (3H, s, CH_3), 1.12 (3H, s, CH_3), 1.09 (3H, s, CH_3), 1.00 (2H, d, J = 15 Hz, 2 ax CH), 0.87 (1H, d, J = 14 Hz, ax CH); TLC, R_f 0.50 (9:1 EtOAc/MeOH).

Anal. Calcd for $C_{23}H_{33}NO_7$: C, 63.43; H, 7.64; N, 3.22. Found: C, 63.24; H, 7.76; N, 3.14.

Kinetic Methods. General. The temperature of the buffer solutions were preequilibrated to either 22 or 37 °C (±1 °C) in the HPLC sample chamber prior to the start of the reactions. HPLC solvents were 0.1% TFA and CH_3CN, and a flow rate of 1 mL/min was used. A Vydac C_{18} column (Catalog no. 218TP54) was employed as the stationary phase. Reactions were initiated by a 1:100 dilution of a stock solution of the reactant into the appropriate buffer. All buffer solutions used were 100 mM buffer/100 mM NaCl. The diode-array detector was set at 280 nm. A 1-μL aliquot from each stock solution was eluted through the HPLC to insure there was no cleavage during the course of the analysis. Elution of 25-μL aliquots from the resulting reaction solutions at various time intervals was used to monitor the course of the reactions. Product and reactant concentrations were determined from the peak area integrations. Based on the observation that the total peak area integrations (starting material + observed product) remained essentially constant (varied by <1%) during the kinetic analysis, it was assumed that the molar absorptivities of the starting material and observed product were identical. The initial concentration of the reactant was calculated by summing the peak areas of the product and unreacted starting material in each chromatogram. For reactions that had half-lives less than 50 h, data were collected over 5 half-lives in order to confirm that the reaction did obey first-order kinetics; for reactions with half-lives greater than 50 h, it was assumed that they obeyed first-order kinetics. The data were fit to a least-squares analysis for the calculation of first-order rate constants.

Kinetics of 6 at 22 °C. A 100 mM stock solution of **6** was prepared shortly before start of the analysis. A Phenomenex Ultremex 3 C_8 column (no. PP/7151D) was employed as the stationary phase. The gradient employed for these analyses ran from 0 to 80% CH_3CN over 25 min. The diode-array detector was set at 260 nm. The retention times for **6** and **8** are 16.0 and 7.1 min, respectively. The pD of the reaction solutions were measured using an Orion Research pH meter 611 and an

Orion Research 8103 Ross combination electrode. pD was calculated by adding 0.4 unit to the pH meter reading. The following deuterated buffers were used: pD 1.0–4.0, sodium chloroacetate; pD 4.0–6.0, sodium acetate; pD 6.0–8.5, sodium phosphate.

Kinetics of 7 by NMR at 22 °C. Analyses were performed on a Bruker AM-400 spectrometer. Dicarboxylate **7** was prepared as described above and used immediately. The buffer solution (995 μL) containing 1,3-benzodioxole as an internal standard was equilibrated for 5 min at 22 °C in the spectrometer, after which it was removed, and to the solution was added 5 μL from the solution of **7**. The resulting solution was quickly mixed and then returned to the spectrometer. Data were collected over time using a program in which each spectra was comprised of 16 scans. The time point for each spectra was taken to be the median point of the spectrum acquisition time. The course of the reaction was monitored at 2.58 ppm for the appearance of the $N-CH_3$ peak of **9**. The following deuterated buffers were used: pD 1.0–4.0, sodium chloroacetate; pD 4.0–6.0, sodium acetate; pD 6.0–8.5, sodium phosphate; pD 8.5–10.0, sodium borate.

Kinetics of 12 at 22 °C. Conditions similar to those used in analysis of **6** were employed, with the following changes. A 100 mM stock solution of **12** in CH_3CN was prepared shortly before start of the analysis. For the analyses performed in D_2O buffers, the stock solution was prepared using CD_3CN. A Vydac C_{18} column (catalog no. 218TP54) was employed as the stationary phase. The diode-array detector was set at 260 nm. The gradient employed for these analyses ran from 0 to 80% CH_3CN over 35 min. The retention times of **12** and **8** were 25.8 and 10.9 min, respectively. The following buffers were used: pD 1.0–4.0, sodium chloroacetate; pD 4.0–6.0, sodium acetate; pD 6.0–8.5, sodium phosphate.

Kinetics of 15 at 22 °C. A 100 mM stock solution of **15** in DMSO was prepared shortly before start of the analysis. The gradient employed for these analyses went from 0 to 64% CH_3CN over 20 min. The retention times of **15** and **18** were 15.8 and 9.0 min, respectively. The following buffers were used: pD 2.0–3.9, sodium chloroacetate; pD 4.0–5.5, sodium acetate; pD 5.6–6.5, MES; pD 6.5–8.0, HEPES.

Kinetics of 15 at 37 °C. Analysis of **15** at 37 °C was identical to the analysis at 22 °C, except that the gradient employed for the analysis went from 0 to 80% CH_3CN over 25 min. The following buffers were used: pH 5.0, 5.5: sodium acetate; pH 5.9: MES; pH 6.3: HEPES.

Kinetics of 16 at 22 °C. A 100 mM stock solution of **16** in CH_3CN was prepared shortly before start of the analysis. The gradient employed for these analyses ran from 0 to 80% CH_3CN over 15 min. The retention times for **16** and **19** were 13.1 and 7.2 min, respectively. The following buffers were used: pD 1.0–4.0, sodium chloroacetate; pD 4.0–6.0, sodium acetate; pD 6.0–8.5, sodium phosphate.

Kinetics of 20 at 37 °C. A 100 mM stock solution of **20** in CH_3CN was prepared shortly before start of the analysis. The gradient employed for these analyses went from 0 to 80% CH_3CN over 25 min. The retention times for **20** and **18** were 16.6 and 9.0 min, respectively. The following buffers were used: pH 5.0, 5.5, sodium acetate; pH 5.9, MES; pH 6.3, HEPES.

Acknowledgment. We thank Julius Rebek and B. Mitra Tadayoni for providing us with the triacids. We also thank D. S. Kemp and John Kozarich for informative discussions. We are also indebted to our colleagues Gary Musso, Phil Friden, Ruth Starzyk, Julie Straub, and Alan Akiyama for their advice and support.